

# We are IntechOpen, the world's leading publisher of Open Access books Built by scientists, for scientists

6,900

Open access books available

186,000

International authors and editors

200M

Downloads

Our authors are among the

154

Countries delivered to

TOP 1%

most cited scientists

12.2%

Contributors from top 500 universities



WEB OF SCIENCE™

Selection of our books indexed in the Book Citation Index  
in Web of Science™ Core Collection (BKCI)

Interested in publishing with us?  
Contact [book.department@intechopen.com](mailto:book.department@intechopen.com)

Numbers displayed above are based on latest data collected.  
For more information visit [www.intechopen.com](http://www.intechopen.com)



---

# The Effect of Impurities in Nickel Grain Boundary: Density Functional Theory Study

---

Iben Khaldoun Lefkaier and El Tayeb Bentría

Additional information is available at the end of the chapter

<http://dx.doi.org/10.5772/66427>

---

## Abstract

By means of density functional theory, we investigate the effect of impurities on structural, electronic and mechanical properties on Nickel  $\Sigma 5$  grain boundary (GB) and its free surface, by studying the effect of 11 transition metal impurities and 8 light elements. The calculation of segregation energy, cohesive energy, formation energy, GB embrittling potency and theoretical tensile strength combined helps us to give accurate conclusions about the effect of these impurities and to compare them with the available experimental and theoretical results. We used the obtained results that are on “equal footing” to establish some correlations and trends. We also confirmed that sulfur and oxygen are the most embrittling elements in Nickel GB in accordance with established literature results and that transition metal elements have a general tendency to segregate to the grain boundaries in a moderate way. Unlike the studied light elements, these elements tend to strengthen the Ni grain boundaries, especially W and Te.

**Keywords:** nickel grain boundaries, DFT, tensile strength, impurities segregation

---

## 1. Introduction

The theoretical investigation of mechanical properties of materials, by means of first-principle calculation and molecular dynamics, has known remarkable advances over the past 15 years [1]. These investigations relate directly to the intergranular behavior, which together with dislocation-based mechanisms determine mechanical response of materials with granular structures. Molecular dynamics calculations can give fundamental understanding of the effects of impurity segregation at GBs in order to predict the mechanical response of materials and their tenability as a function of alloying additions. On the other hand, first-principles calculations

---

can be quite effective in developing this understanding. We can assess whether an impurity is a cohesion enhancer and causes the strengthening of the GB or is an embrittler and induces the weakening of the GB, while experimental techniques are difficult to investigate one impurity alone without the influence of other impurities.

First-principle calculations are widely used for metals and alloys. Grain boundaries of iron make a large part of these investigations. Impurity segregation to the GB in iron is described and understood relatively well, both theoretically and experimentally. In contrast, this is not the case of GB in nickel. The experimental information is quite rare [2]. In recent years, many efforts have been devoted to theoretically determine the effect of impurities on nickel grain boundaries, motivated by the industrial challenges facing fabrication and aging of nickel-base superalloys [3].

It is already well known, both experimentally and theoretically, that sulfur acts as an embrittling element in nickel grain boundary and boron acts as enhancing element [3]. Some other elements like phosphorus are not that clear from first-principle calculations and became a subject of debate between strengthen and embrittling [4]. In contrast to light elements, influence over Ni grain boundaries of alloying elements took less attention [5]. The main elements for this purpose are transition metals, and the most important of them are elements of columns IV–VII and periods 4–6 of the periodic table.

Even though some of these element impurities effects have been studied theoretically, it is remarkable that there are still no comparisons between the effects of these element in the GB. This is because it is hard to make comparison between results of different works due to the differences in impurity concentrations, GB models, number of atoms per unit cell, methods of calculations and type approximations used. We think that it is important now to have a systematic study to find the most enhancing and the most embrittling elements on Ni GBs. This knowledge can be used also to optimize the material properties as we are trying to understand the mechanisms and effects of different impurity atoms.

This chapter is divided in two parts. Part I is about the methodology of our calculations. Part II describes and discusses the obtained results, and it is organized as follows. First, details of calculation of the effect of Vanadium and Niobium in Nickel GB are exhibited. The effect of light elements “B, P, O, N, Al, Si, S, C” in Ni $\Sigma$ 5 GB and surface and also of transition metal elements “Ti, V, Cr, Mn, Zr, Nb, Mo, Hf, Ta, W, Re” in Ni $\Sigma$ 5 GB and surface are presented and discussed. Finally, a main conclusion is drawn.

## 2. Model, methods and computational details

This chapter describes the Nickel  $\Sigma$ 5(210) grain boundary models used in these work. Since we are dealing with 2D defect, the constructed structure is not evident as crystals. Beside this, computational parameters used in different models are presented with the precision required and explanation the choice of methods of calculations and the adequate approximations. We briefly present how to calculate free surface energy, grain boundary energy and the tensile strength for a clean and impurity decorated GB.

## 2.1. Computational details

Total energy calculations and geometry optimizations have been carried out using pseudo-potentials plane-wave method as implemented in Cambridge serial total energy package (CASTEP) [6].

Local density approximation LDA CA-PZ is used for the exchange-correlation potentials (CA-PZ: Ceperley-Alder [7], data as parameterized by Perdew and Zunger [8]). Norm-conserving pseudopotentials (NCP) [6] are used with 720 eV plane-wave cutoff energy for all calculations. The valence electronic configuration of Ni is  $3d^84s^2$ , and all other transition metal elements are treated including the d shell in valence bonds. The k-points sampling of Ni unit cell was carried out using  $8 \times 8 \times 8$  Monkhorst Pack mesh grid, which corresponds to different sampling on different model such as  $4 \times 4 \times 1$  k-points sampling for the 22 and 80 atom model and  $3 \times 5 \times 1$  for the 44 atom model of our grain boundaries. **Figure 1** presents a sample of 44 atom model used in segregation energies; substitutional segregation sites are sited from 1 to 11. This optimized values lead to an acceptable accuracy for the calculation of the total energy since we are calculating only the difference in total energy between two calculations; thus, a precision of 1 meV is sufficient. In the calculation of density of state and Mullikan population analyses which depend on the derivative of the total energy, we used more strict tolerance such as  $6 \times 6 \times 2$  in k-point sampling. The calculations assure a high level convergence of the total energy difference with respect to the number of atoms within  $10^{-6}$  eV for total energy and maximum Hellmann-Feynman force within 0.1 meV/Å for pure Ni  $\Sigma 5(210)$  GB and energy difference of  $2 \times 10^{-5}$  eV per atom for segregation and tensile test calculations.

For reasonable and fast convergence of the total energy, electronic occupancies were determined according to a Gaussian scheme with an energy smearing of 0.2 eV. The Pulay scheme of density mixing was used for self-consistent field (SCF) calculations [9].

In this work, we are dealing with Nickel GBs and transition metal impurity mainly, and they provide unique challenges to compute the electronic structure and for some pseudopotentials cause a lot of trouble to converge to an acceptable criteria. The choice of LSDA, norm-conserving pseudopotentials, came after a long study; we have done based mainly of the convergence of the total energy.

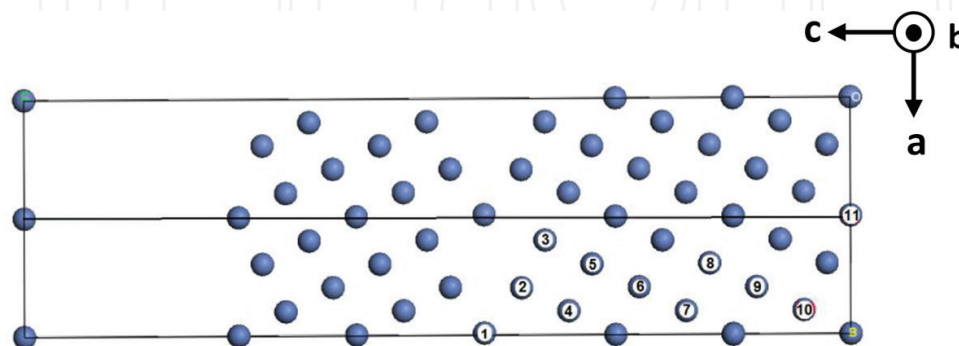


**Figure 1.** Unit cell model of Ni  $\Sigma 5(210)$  symmetrical tilt grain boundary, model used in segregation study. Unit cell shapes are shown by solid lines. Axes directions and orientations are also presented. Atomic sites used in segregation are indicated by numbers (0–11).

Ultrasoft	$a$ (Å) Spin	$a$ (Å) Non-spin	Magnetic moment $\mu$	Norm-conserving	50 SCF step (s)
LDA CA-PZ	3.516	3.451	0.740	LDA	2077.780
GGA-PBE	3.553	3.547	0.660	LSDA	7875.180
GGA-PW91	3.550	3.544	0.640	X-time	3.790
Exp	3.524			Ultra-soft	
NC-PP	Spin	Non-spin	Magnetic moment $\mu$	LDA	2057.780
LDA CA-PZ	3.518	3.506	0.760	LSDA	7851.480
GGA-PBE	3.451	3.440	0.720	PAW-LSDA	2404.180
GGA-PW91	3.430	3.443	0.680	28kpt-600	

**Table 1.** Nickel lattice parameters in Å with different computational parameters for the magnetic and nonmagnetic case, and the time in seconds for the first 50 SCF cycle for different LDA combinations using 4 cores 3.4 GHz.

**Table 1** presents the calculated lattice parameters for Nickel single crystal for different pseudopotentials and methods. As expected, for both approaches “ultrasoft and norm-conserving,” LDA underestimates the lattice parameter 3.524 Å and the GGA overestimates it. The error for all methods is acceptable and has a maximum value of 2.66%. Moreover, the non-spin treatment results shrinking of lattice parameter. The method that most predict the lattice parameter is LSDA using norm-conserving pseudopotentials with error of 0.17%.

From **Table 1**, we can also see the CPU time cost for 50 SCF steps using four cores 3.4 GHz and 32 GB RAM. The spin treatment costs about four times that the non-spin calculations, which explains why many calculations in the past were expensive to perform with spin treatment, particularly when the lattice parameters have close values. In order to compare the CPU time used in this work, we perform calculation with the “PAW method” implemented in VASP package, which is the most used method for GBs calculation in Ni. We use the same GB model with the closest parameters. The result shows that PAW is about two to three times much faster than norm-conserving.

We have to mention that the choice of LSDA using norm-conserving was not based mainly on lattice parameters nor on CPU time, but on convergence of total energy for transition metal element, especially during tensile test. The majority of other conducted methods fail to converge when the separation distance between the two surfaces is larger than 3 Å “during tensile test.” Norm-conserving with LSDA was the best combination that converges well to the required tolerance in all cases.

## 2.2. Fundamental grain boundaries parameters

### 2.2.1. Grain boundary and free surface energies

We introduce the GB energy ( $\gamma_{GB}$ ) and free surface (FS) energy ( $\gamma_{FS}$ ) to characterize GB cohesive properties, which are defined as the energies needed to create a GB and FS in the bulk [10]. They are given by the following relations:

$$\gamma^{GB} = \frac{E_{tot}^{GB} - E_{tot}^{Bulk}}{2S^{GB}} \text{ and } \gamma^{FS} = \frac{E_{tot}^{FS} - E_{tot}^{Bulk}}{2S^{FS}} \quad (1)$$

where  $E_{tot}^{GB}$ ,  $E_{tot}^{FS}$  and  $E_{tot}^{Bulk}$  are total energies of the GB, FS and bulk system, respectively, and  $S^{GB}$  and  $S^{FS}$  refer to GB and FS areas in the GB model. In order to obtain all energies on equal footing and to make suitable comparisons, the calculations of  $E_{tot}^{Bulk}$  and  $E_{tot}^{FS}$  for the unperturbed Ni FCC ferromagnetic are performed with equal number of atoms per model.

### 2.2.2. Segregation and binding energies

The impurity segregation energy is defined as the difference between the total energy of a system  $E_{I-FS/GB}$  with the impurity in the surface layer (or GB), and the energy  $E_{Bulk}$  with the impurity is in the bulk:

$$E_{I/GB} = E_{I-FS/GB} - E_{Bulk} \quad (2)$$

Therefore, the sign convention is that the negative segregation energy corresponds to impurities that want to segregate [5].

According to the Rice-Wang model [11], the binding energies of the impurities at the grain boundary  $\Delta E_b^{GB}$  are defined as follows:

$$\Delta E_b^{GB} = E_{I/GB} - E_{GB} - E_I \quad (3)$$

where  $E_{I/GB}$  is the total energies of the GB system with segregated impurity atoms,  $E_{GB}$  is the energy of clean GB system, and  $E_I$  is the energy for one isolated impurity atom. The larger negative value of the binding energy of the impurity at the GB means stronger bonding between the impurity and nickel atoms.

So in order to calculate these two properties (segregation and binding energies), we need to use six models which are:

- Fully relaxed clean grain boundary,  $E_{GB}$ .
- Fully relaxed grain boundary with segregated impurity atoms,  $E_{I/GB}$ .
- Fully relaxed clean grain boundary with the impurities deep in the bulk region,  $E_{I/GB,bulk}$ .
- Relaxed clean free surface,  $E_{FS}$ .
- Relaxed free surface with segregated impurity atoms,  $E_{I/FS}$ .
- A monolayer of impurity atoms,  $E_I$  in positions which correspond to the impurity atoms at the grain boundary.

### 2.2.3. Theoretical tensile strength

The theoretical (ideal) strength of a crystal as defined by reference [12] is determined by “the maximum stress at elastic instability (yield or break) when applying an increasing stress to an infinite perfect crystal. It forms an upper limit to the strength of a real crystal (**Figure 2**), which is of both scientific and engineering value. The theoretical strength is an intrinsic material property, which is

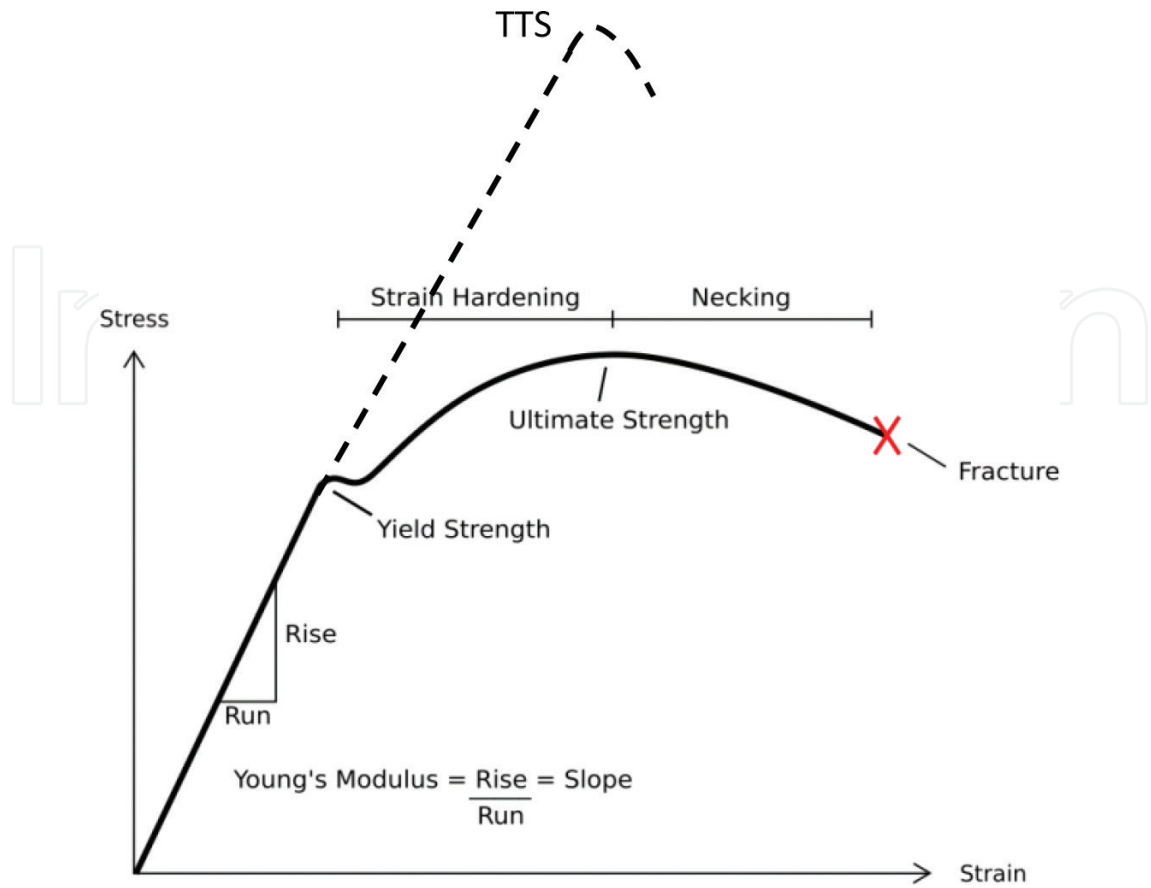


Figure 2. Typical stress vs. strain diagram indicating the various stages of deformation, open source image (modified).

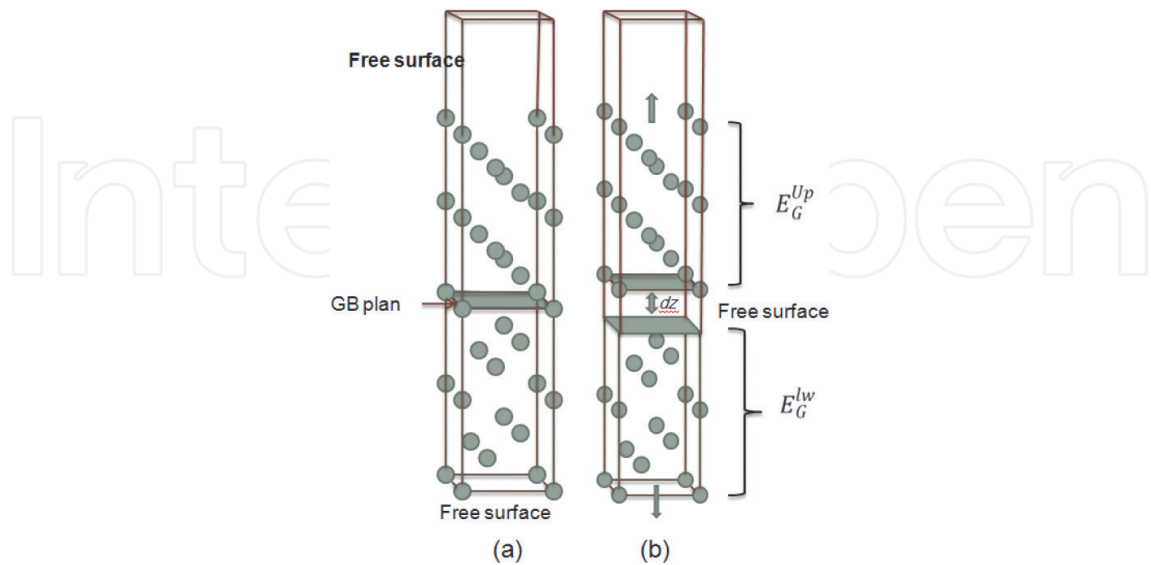


Figure 3. Representation of the GB fracture, the GB is separated in the weakest region, which corresponds to the (210) surface that attach the two grains, dz presents the separation distance.

determined by the behavior of valence electrons and ions. Similarly, the theoretical strength of an ideal defective system containing only one defect such as a point defect, an interface, a grain boundary, etc., can be determined as the maximum stress required to reach elastic instability under increasing load without introducing extrinsic dislocations or cracks" (Figure 2) [12].

Here, we recall how to calculate the cohesive energy  $2\gamma$  and the tensile strength  $\sigma_{\text{Max}}$  (equal to the maximum tensile stress), as presented in [13]. We set a fracture plane that gives the minimum cohesive energy; then, the upper and lower half crystal blocks are rigidly separated by five equal increments (Figure 3). Each time in the separation process, we perform structure relaxation of the GB region, while fixing atomic layers close to the free surface in order to mimic the bulk structure. Then, the cohesive energy  $2\gamma$  of the GB is the difference between the two total energies:

$$2\gamma = E_{\text{GB}} - E_{\text{S-GB}} \quad (4)$$

$E_{\text{GB}}$  is the energy of the GB without separation (point 0), and  $E_{\text{S-GB}}$  is the total energy for which the separating distance is so large that it does not change any more, typically after 0.5 nm separation.

The maximum tensile stress is calculated as follow. A simple function  $f(x)$  is fitted to the calculated total energy versus separation distance  $x$

$$f(x) = 2\gamma - 2\gamma \left(1 + \frac{x}{\lambda}\right) \exp\left(-\frac{x}{\lambda}\right). \quad (5)$$

Here  $2\gamma$  and  $\lambda$  are fitting parameters.  $\lambda$  is defined as the Thomas-Fermi screening length. This function is known as the universal binding curve proposed by Rose et al. [14]. It describes well the bonding nature between atoms and constitutes the best fit of binding energies versus atomic distances for the metallic systems. The tensile stress is the derivative of  $f(x)$ :

$$f(x) = \frac{2\gamma x}{\lambda^2} e^{-\frac{x}{\lambda}}$$

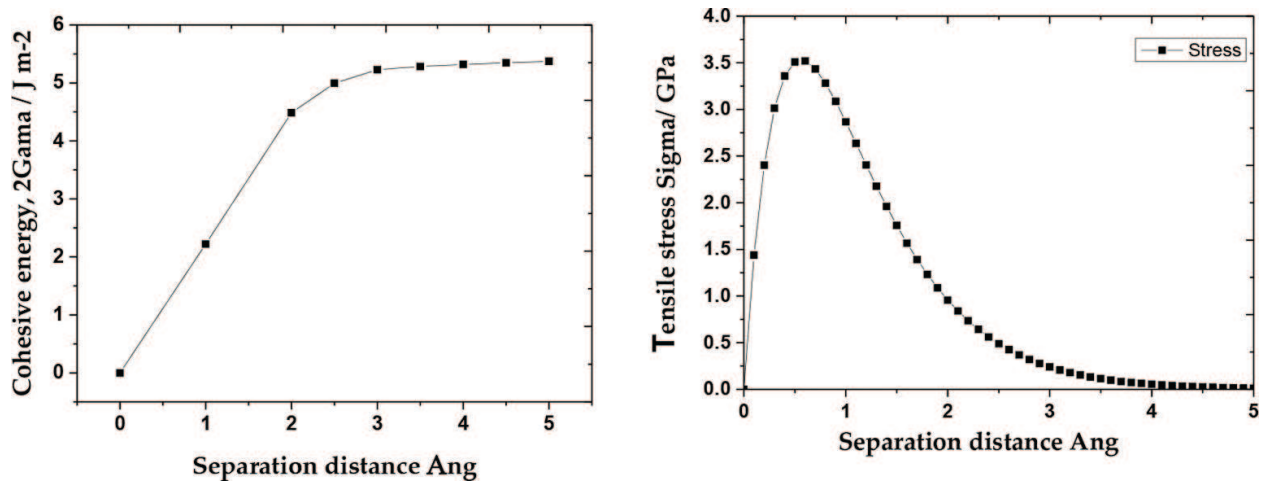


Figure 4. The variation of cohesive energy and tensile stress for FeΣ3(111) GB with boron impurity segregate in site 0.

The maximum of  $f(x)$  is at  $x = \lambda$  and corresponds to the maximum theoretical tensile stress or tensile strength  $\sigma_{Max}$ ; therefore,

$$\sigma_{Max} = f(\lambda) = e^{-1} \frac{2\gamma}{\lambda} \quad (6)$$

The **Figure 4** represents a calculated example that shows the variation of total energy in Fe  $\Sigma 3(111)$  GB with boron impurity segregate in site 0, and the value of the  $2\gamma$  is  $5.41 \text{ J m}^{-2}$ ; thus, the cohesive energy  $\gamma$  is  $2.70 \text{ J m}^{-2}$ . The tensile strength is plotted by evaluating the derivative of Rose function  $f(x)$  with function of separation distance  $x$ .

### 3. Results and discussion

#### 3.1. Nickel $\Sigma 5$ STGB

In order to verify whether the present GGA norm-conserving pseudopotentials (NCP) basis sets are suitable to our Ni GB model, we calculated surface and grain boundary energies presented in Eq. (1) of Nickel GB and compare them with known results of previous experimental and theoretical works (**Table 2**). Indeed, our result agrees well with both experimental results and previous theoretical calculations (see **Table 2**). Thus, we have a strong confidence in the constructed GB configuration of this work.

The calculated total DOS (TDOS) for the grain boundary model (**Figure 5**) appears to have similar characteristics to that of the bulk, that is, the trend of the plot and the density of electrons values are close to each other, and also that the d-bonds are the responsible for bonding, which means that there is no major change in the metallic bonding.

Now we study the difference between Ni atom in perfect bulk and Ni atom in the GB region. From **Figure 5**, we take site 1 as example, because it represents well the different in environments, and we remark that there is a DOS shape compression of the Ni at GB. The difference is much remarkable for the d states that vary from  $-5$  to  $+3$  eV for Ni in the bulk and narrowed for the site1 from  $-5$  to  $+0.5$  eV (**Figure 5**). This compression happened more in the conduction which mean that the GB region reduces electric conduction (barriers) because we know that the electric conduction depends on the electron density around Fermi level [15].

Chen et al. [16] calculate partial DOS (PDOS) for different layers and show that the GB has a significant effect on the shape of d-DOS, and show that at layer 4 the d-DOS became indistinguishable from that calculated for the bulk atom; we could conclude that the effect of the grain boundary in Ni binding disappears totally in the 4th layer.

J.m <sup>-2</sup>	Our NCP	PP-PAW	US-GGA	Exp. (polycrystal)
GB energy	1.23	1.23 <sup>a</sup> , 1.43 <sup>b</sup> , 1.33 <sup>c</sup>	1.41 <sup>e</sup>	0.93 <sup>d</sup> , 1.24 <sup>f</sup>
FS energy	2.53	2.34 <sup>a</sup> , 2.65 <sup>b</sup> , 2.29 <sup>c</sup> .	2.40 <sup>e</sup>	2.59 <sup>d</sup> , 2.02 <sup>f</sup>

a Ref. [18]. b Ref. [20]. c Ref. [13]. d Ref. [5]. e Ref. [29]. f Ref. [30].

**Table 2.** Calculated grain boundary (GB) energy and free surface (FS) energy of Ni  $\Sigma 5(210)$  GB (in  $\text{J m}^{-2}$ ) [28].

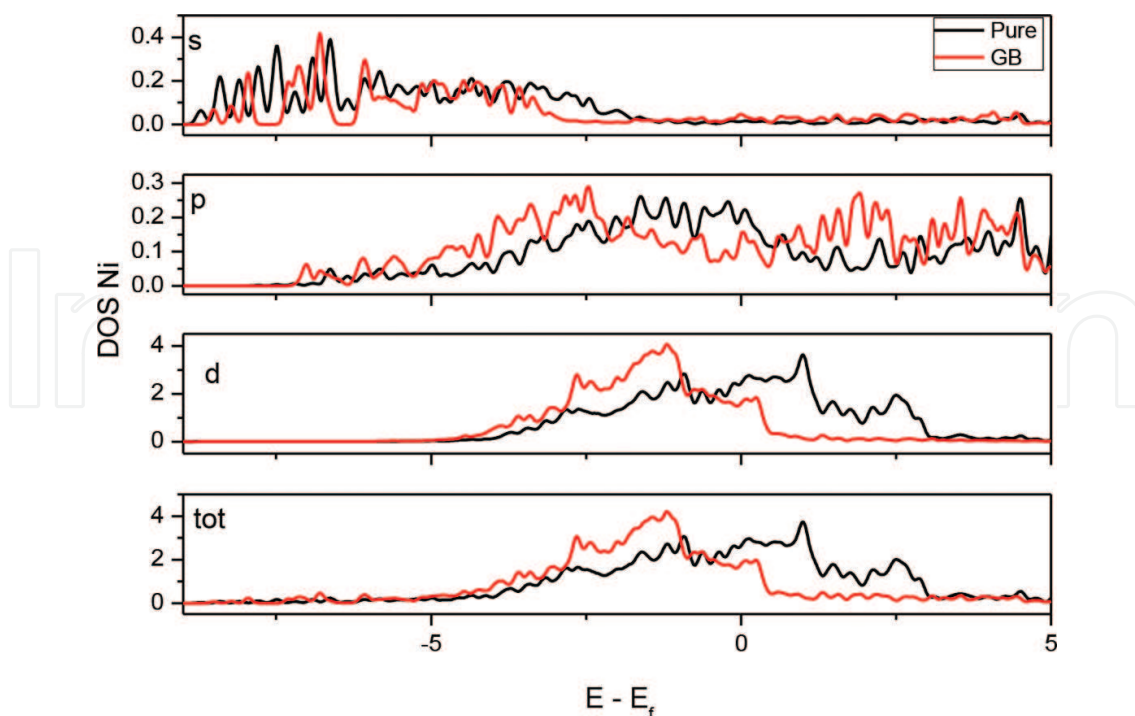


**Figure 5.** Total and partial density of states for Ni atom in bulk and in site 1 of the grain boundary.

In both cases, the magnetic moments of Ni increase when we move from GB until it reach the bulk value from the 6th layer on [10], which is also remarked here.

### 3.2. The effect of light elements “B, P, O, N, Al, Si, S, C” in Ni $\Sigma$ 5 GB

In this part, we discuss our results of tensile strength which is uncovered topic for these eight light elements except B and S which is already calculated [17, 18]. We compare our results of segregation and binding energy with the available experimental and theoretical calculations.

#### 3.2.1. Phosphor impurity effect

Controversy regarding the role of P in the Ni GB, Geng et al. [19] proved that P is an embrittler to Ni GB by means of atomic distances, electronic structures and the RWEF. In contrast, Masatake et al. [20] declared that P has a beneficial effect on the Ni GB cohesion, which is in contradiction with previous calculations. While Všíanská et al. showed that interstitially segregated P has none or negligible strengthening effect on Ni GB by studying the RWEF. Liu et al. [4] decide to reach a more profound conclusion by calculation of phosphor effect with function of concentration. They found that when the concentration of P is relatively low (0.25–0.5 monolayer, i.e.,  $N_p = 1-4$ ; **Figure 6**), P tends to bond strongly with the neighboring Ni atoms, which is beneficial to the GB cohesion.

In the meanwhile, P draws charge from these Ni atoms and removes electrical charges from the Ni–Ni bonds to weaken them. As the P concentration increases ( $N_p = 5-7$ ), P atoms get close and exert a repulsive interaction on each other, thus result in a thin and fragile zone in

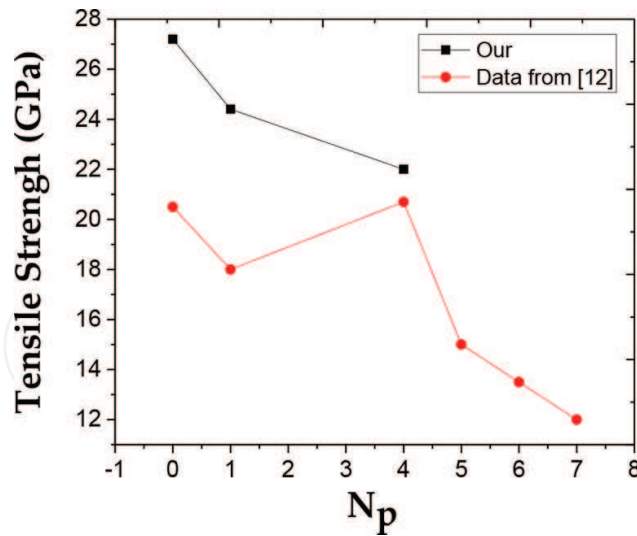


**Figure 6.** The variation of TTS with function of concentration. The case of  $N_p = 1$  represents the GB with 1 P atom in layer 0 or 2, and the case of  $N_p = 4$  represents the GB with 4 P atoms in layer 0 or 2. In the range of  $N_p = 5-7$ , layer 0 is fully occupied by 4 P atoms and layer 2 is occupied by 1-3 P atoms, data from Ref. [4].

the GB. Our calculation corresponds to configuration 2P ( $N_p = 2$ ) corresponding to 0.5 atom/ML at GB see [4], which is favorable from the energetic point of view of Liu (**Figure 6**). The largest segregation energy in Liu is  $-1.45$  eV correspond to 4p concentration. This value is in agreement with ours about  $-1.77$  eV for 1p concentration. The results of tensile strength are different from ours due to the different methods and approximation used for TTS calculation. Moreover, our results for segregation energy are much closer to Všíanská et al. ( $E_{seg} = -1.6$  eV). We found that P has embrittlement effect for this concentration, with positive RWEF, confirmed by the value of TTS (24.4 GPa) and with little decreases of cohesive energy to 3.44 eV. For concentration 4P ( $N_p = 4$ ) (1atom/ML), we calculate the TTS, appear to be much lower than Liu value and correspond to 22 GPa with cohesive energy of 3.3 eV that confirm the increase of the embrittlement effect with the increasing of the P concentration. Our results for two P concentrations show that there is no enhancing effect of phosphor impurities and acts always as embrittler.

### 3.2.2. Oxygen and sulfur impurity effect

Oxygen and sulfur have very destructive effect on the Ni GBs. This is clear from tensile strength values presented in, which reduce TTS by 23%. Sulfur is always considered as the most damaging embrittler due to its inevitable existence sometimes in industrial processes. Many experimental and theoretical studies were carried out about its effect [10, 13]. In the other hand, oxygen didn't get that attention at least for theoretical calculation. Here we try to focus more on the effect of oxygen and mention some literature reviews.

Our results show that oxygen impurity present a clear embrittlement to the Ni GB, with the strongest reduction in the cohesive energy that reaches  $3.08$  J/m<sup>2</sup> of Ni GB. The TTS presents a value of 21.1 GPa and the largest RWEF (1.48 eV/atom). Všíanská and Šob [10] explain that by the fact that isolated oxygen atom has a large magnetic energy, which is the reason for making

the binding energy of oxygen very large and cause a GB expansion which leads to embrittlement. Furthermore, some experimental observations about the effect of oxygen in NBS by Bricknell and Woodford [21] describe some results and observations on air embrittlement of a commercially pure nickel (Ni200) and show that oxygen was the damaging species and that nitrogen was innocuous. They mention that *“the high concentration of sulfur at the boundaries made oxygen detection by Auger analysis extremely difficult. However, direct evidence for grain boundary oxygen penetration was provided by the formation of various oxygen containing compounds, which were readily observed using scanning electron microscopy”* [21].

Yamaguchi et al. [13] perform comparison between calculated tensile strength for different sulfur impurity concentrations and compare them with experimental ultimate tensile strength with the same concentration of FCC Ni GB [13]. One can see that the order of the tensile strength largely differs between experiment and calculation, and both of strengths are reduced by one order of magnitude with increasing sulfur concentration [13]. The discrepancies in values are due to many reasons. The most plausible of them is the fact that DFT simulations are done for a small model of one symmetrical tilt grain boundary without taking in account the dislocations, while experimental fracture occurs at various kinds of grain boundaries (random grain boundaries, etc.) associated with dislocation emitting. Considering these facts, the agreement between behavior of TTS calculations and experiments seems to be reasonable.

### 3.2.3. Boron impurity effect

Masatake et al. [20] have calculated the embrittling potency energy of some light elements and show that boron has the best enhancing value for these impurities. This is also the case here. Later then, with 80 atom Ni FCC model, Kart and Cagin [18] investigated the effects of boron segregation at the Ni  $\Sigma 5(210)$  GB in the four interstitial possible positions. They found that increment of the boron atom in the GB site 0 increases the value of the theoretical tensile strength for Ni. Using GGA approximation, they show that the stresses for the GB including one, two, three and four boron atoms are evaluated as 24, 26, 25.8 and 27 GPa, with 23 GPa for the pure GB. Our calculations are relatively in a good agreement, with 37.6 GPa for two boron atoms in GB and 27.6 GPa for the pure Ni GB. The difference in TTS results is due essentially to different TTS calculation methods, which is with GGA approximation known to give lower TTS value than our method approximation (LSDA). All these works agree together that boron is an enhancer to Ni GB. In our calculation, boron presents the highest tensile strength and also the highest RWEF of  $-0.94$  eV. This makes him the best impurity type in the considered eight light elements.

### 3.2.4. Aluminum and silicon impurity effect

These two elements are juxtaposed on the same column, that is, they have the same electron number in valence band. These elements take the less attention in the computational side due to their indecisive effect and controllability of their existence in experiments [22].

Geng et al. [19] have expect that aluminum and silicon, which have similar atomic size and bonding as phosphorus, would be embrittler for Nickel  $\Sigma 5(210)$  GB. Later on, Všianská and

Šob [10] have calculated the segregation energy and embrittlement potency and show that, contrary to the Geng prediction, Si acts as enhancer with Rice WEP  $-0.41$ , and Al has no significant effect in Ni GB with RWEPE  $-0.03$ .

For Silicon, our results confirm Šob findings, but they go more to Geng prediction for Al which presents more embrittlement character with RWEPE  $+0.16$ . Beside Geng and Šob approaches, our results expected to be more accurate with the calculation of the cohesive energy and the TTS, which show embrittlement of Al impurities to  $24.6$  GPa, and a little enhancement of Si impurity to  $28.2$  GPa, and validate the RWEPE values.

### 3.2.5. Carbon and nitrogen impurity effect

Siegel and Hamilton [31] have studied carbon segregation and diffusion within a Nickel  $\Sigma 3$  grain boundary and show that interstitial site is preferred for the magnetic and nonmagnetic cases. But the author did not calculate the strengthen effect. In 2008, Sanyal et al. [23] have talked about the strengthen effect of carbon impurity in Nickel  $\Sigma 5(210)$  GB using the cohesive energy values. They founds decres of the cohesive energy from  $3.60$  to  $3.54$  eV, in which they concluded that C acts as embrittler. Using a 20 atoms model, Masatake et al. [20] have found negative RWEPE which means that C acts as cohesive enhancer. Contrarily, Young et al. [24] find positive RWEPE with 40 atom models which confirm that C is an embrittler impurity. This result is in agreement with our  $2 \times 2 \times 64$  atoms model, in which we found enhancement in cohesive energy, TTS and negative RWEPE. This controversy in results is mainly due to the model number of atoms, and thus, we confirm the remark of [25] that low segregation energy can give wrong values.

For the Nitrogen case, we found that N impurity atom results a positive RWEPE and a lower cohesive energy, but with a small enhancement in the TTS. This value of TTS is not in agreement with the RWEPE and cohesive energy. RWEPE results in [20] agree well with our RWEPE finding for the non-spin calculation, taking into account the loose in cohesive energy of a GB with N impurity. Taking in to account the result of Masatake and as mention above that the total energy and forces of some elements mainly for N do not converge to the required criteria for some fracture cases, we can conclude based only on the two factors (RWEPE and  $E_{coh}$ ) that N is embrittler.

### 3.2.6. General tendency

Young et al. [24] have put the order of the impurities effect from most embrittling to most strengthening, the impurity elements are ranked as He, Li, S, H, C, P, Fe, Mn, Nb, Cr, and B. Helium is strongly embrittling ( $+1.07$  J/m<sup>2</sup> lowering of the RWEPE), while phosphorus has little effect on the grain boundary ( $-0.05$  J/m<sup>2</sup>), and boron offers appreciable strengthening ( $-0.54$  J/m<sup>2</sup> increase in RWEPE). These findings are consistent with experimental observations (e.g., He, S and H are known embrittling agents and boron is a known strengthener in nickel-base alloys). This classification is in excellent agreement with our tensile strength results even the paper was conducted on  $\Sigma 5$  twist Ni GB along, which give us more confidence that the study of the effect of impurity in one type of GB could lead us to general result about its behavior in other type of Ni GBs.

### 3.3. The effect of transition metal elements “Ti, V, Cr, Mn, Zr, Nb, Mo, Hf, Ta, W, Re” in Ni $\Sigma$ 5 GB

Light elements are, in general, known as embrittling agents for Nickel, whereas transition metal elements are known as the main enhancing alloying impurities. Even though these elements have been subject of intensive thermodynamic based studies for their effects on Nickel as impurities, there is a lot of discrepancy in results of different models [19]. Nevertheless, there are few works which treat it by quantum mechanical approaches [23, 24]. Razumovskiy et al. [5] calculated the segregation energy, partial cohesive energy and RWEF for W, Zr, Hf, Bi, S, B, Ta and Re. While writing this work, another work from Ref. [3] conducts a study of purpose to the design of Ni-base polycrystalline superalloys by studying the influence of a wider range of transition metal elements on grain boundary segregation and bulk cohesion in Ni  $\Sigma$ 5(210) GB.

In this paragraph, we compare and discuss the results of segregation energy and tensile strength for some elements mentioned in other works. Hf impurity shows an important RWEF of  $-0.61$  in agreement with Razumovskiy et al. value of  $-0.69$  eV/atom. Sanyal et al. [23] found that Hf was favored at the GB by  $+0.8$  eV/atom relative to that in the bulk. Hf is experimentally found to strengthen GBs [26]. In this work, we add more information about its effect by TTS calculation. We predict that Hf is not a good enhancer if available alone in the GB. Its existence in Ni GB with other embrittling elements such as sulfur further should be studied. The high segregation energy of Hf may compete S segregation to Ni GB and overcome its undesired effect.

Ta has the highest RWEF among transition metals with a large cohesive energy of  $+5.22$  eV and second largest TTS after W. Ta is hence one of the best enhancer. We found a negative and large value of segregation energy at GB for Ta  $-0.91$  eV. Similar conclusion was also drawn by [5].

If we refer to our calculated results about Cr additions, this element does not prefer to be at the GB region, but rather to the surface. Even though, it presents a positive RWEF. Its effect in the GB if existed is not harmful and doesn't affect considerably the cohesive energy and TTS calculations. The later result is confirmed by the small negative RWEF value of Cr in Young work [24].

W has the largest cohesive energy, the highest TTS and a very important RWEF. Based on these factors, we can say that W is the best enhancer among the 12 considered transition metals elements with small difference with Ta. Represents high cohesive energy, but it does not have the highest tensile strength, in accordance with Tahir's work [27] that cohesive energy does not give full presentation of enhancement/embrittlement.

Based on other first-principles method calculations (full-potential linearized augmented plane-wave method FLAPW). Geng et al. [19] calculated that the cohesive energy for all transition metals elements in order to, unambiguously, predicts the effect of a substitution alloying addition on grain boundary cohesion of metallic alloys. **Figure 7** presents a comparison between our calculated values for the cohesive energy and those obtained by Gang et al. [19]. We notice that even there is a similar trend in both results (e.g., W has the largest cohesive

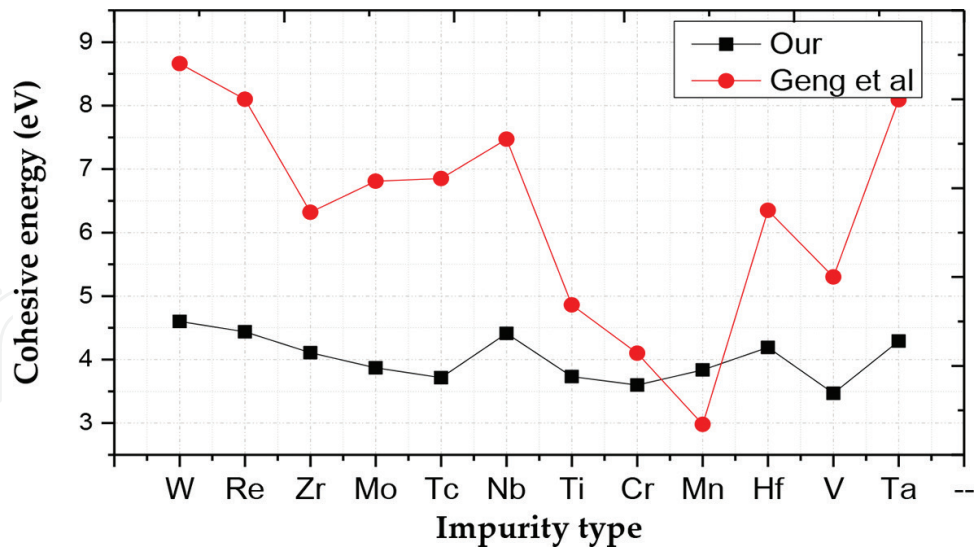


**Figure 7.** The cohesive energy of Nickel  $\Sigma 5$  GB with impurity type in it, element in X axes represents the impurity type (one atom) generally located on Site1. Data 1 taken from Ref. [19].

energy followed by Re and Ta approximately with the same value and so on), and the cohesive energy values are quite different. **Figure 7** shows that the cohesive energy from our calculations varies in the range [+5.6 to +4.6 eV], while Geng results fluctuate largely from +8.66 to +2.98 eV. Geng results seem to be less accurate than ours. For example, Geng calculated cohesive energy for W impurity at Ni GB and found 8.66 eV, 2.4 time larger than our value and other known pure GB cohesive energies [19]. This value (8.66 eV) could lead to very high value of tensile strength equal to 65 GPa and vice versa 22 GPa for Mn (lower than sulfur), which are simply not reasonable for the magnitude range of Ni-TTS. We think that these fluctuations are first due to the number of atoms (22 atoms) in Geng model, which leads to highest segregation energies and therefore higher effect on the GB TTS. Also, the relaxation of atomic positions was only done in the normal direction to the GB plane and ignored in both lateral and the mirror symmetries in the normal direction to the GB plane (210).

#### 4. Conclusion

In this work, we conduct analyses about the influence of segregated impurities on the properties of nickel grain boundaries. The problematics and controversy of results posed here have a dual character: fundamental and industrial. The selected impurities are eight light elements and eleven transition metals elements of the periodic table. The adopted methodology for this study was based on density functional theory widely used in recent years to predict the mechanical response of materials and their tenability as a function of alloying additions.

After optimization study, we have shown that the norm-conserving approach together with local density approximation is best suited to solve convergence problems as well as to give accurate results in the case of metallic systems. Furthermore, different GB models have been used in order to fulfill the required calculated property.

Calculations permitted us to confirm that light elements (column 13–16, periods: 2 and 3) have strong tendency to segregate at Ni grain boundary due to their small size and high electronegativity. However, their influence on the cohesion of the grain tensile strength (TTS) differs from one element to another. We also confirmed that sulfur and oxygen are the most embrittling elements in Nickel GB in accordance with established literature results.

Our calculations show that the transition metal elements (column 22–25 periods: 4–6) have a general tendency to segregate to the grain boundaries in a moderate way. Unlike light elements, these elements tend to strengthen the Ni grain boundaries, with the exception of Mn which acts as embrittler, in which we studied further in order to explain this case. We have shown that the magnetism of Mn plays an important role in the GB decohesion. Among these transition elements, we have shown that W and Re are the most consolidating for Ni GB and therefore are candidates for counter embrittlement of sulfur.

## Author details

Ibne Khaldoun Lefkaier<sup>1</sup> and El Tayeb Bentria<sup>2\*</sup>

\*Address all correspondence to: [ik.lefkaier@lagh-univ.dz](mailto:ik.lefkaier@lagh-univ.dz)

1 Materials Physics Laboratory, University of Laghouat, Laghouat, Algeria

2 Qatar Environment and Energy Research Institute (QEERI), Hamad Bin Khalifa University, Doha, Qatar

## References

- [1] Erich, W., N. Reza, A. Y. George, Jr., D. B. Jake, M. A. Thomas, V. James, J. C. James, N. Hiroaki, B. S. Judy, F. Clive, C. Mikael, W. Walter and S. Paul. Ab initio calculations for industrial materials engineering: successes and challenges. *Journal of Physics: Condensed Matter*. 2010;**22(38)**:(384215).
- [2] Všianská, M. Electronic structure and properties of grain boundaries in nickel. Diss. Masarykova univerzita, Přírodovědecká fakulta. 2013.
- [3] Razumovskiy, V. I., A. Y. Lozovoi and I. M. Razumovskii. First-principles-aided design of a new Ni-base superalloy: Influence of transition metal alloying elements on grain boundary and bulk cohesion. *Materials Science and Engineering A-structural Materials Properties Microstructure and Processing*. 2015;**107**:(23–40).
- [4] Liu W., C. Ren, H. Han, J. Tan, Y. Zou, X. Zhou, et al. First-principles study of the effect of phosphorus on nickel grain boundary. *Journal of Applied Physics*. 2014;**115**:(043706).
- [5] Razumovskiy, V. I., A. Y. Lozovoi, I. M. Razumovskii and A. V. Ruban. Analysis of the alloying system in Ni-base superalloys based on ab initio study of impurity segregation to Ni grain boundary. *Advanced Materials Research*. 2011;**278**:(2011):(192–197).

- [6] Clark Stewart, J., D. Segall Matthew, J. Pickard Chris, J. Hasnip Phil, I. J. Probert Matt, K. Refson and C. Payne Mike. First principles methods using CASTEP. *Zeitschrift für Kristallographie*. 2005;**220**:(567).
- [7] Ceperley, D. M. and B. J. Alder. Ground state of the electron gas by a stochastic method. *Physical Review Letters*. 1980;**45**(7):(566–569).
- [8] Perdew, J. P., A. Zunger. Self-interaction correction to density-functional approximations for many-electron systems. *Physical Review B*. 1981;**23**:(5048–79).
- [9] Pulay, P. Ab initio calculation of force constants and equilibrium geometries in polyatomic molecules: I. Theory. *Molecular Physics*. 1969;**17**(2):(197–204).
- [10] Všíanská, M. and M. Šob. The effect of segregated sp-impurities on grain-boundary and surface structure, magnetism and embrittlement in nickel 817-840. *Progress in Materials Science*. 2011;**56**(6):(817–840).
- [11] Rice, J. R. and J. S. Wang. Embrittlement of interfaces by solute segregation. *Materials Science and Engineering: A*. 1989;**107**:(23–40).
- [12] Lu, G. -H., et al. Theoretical tensile strength of an Al grain boundary. *Physical Review B*. 2004;**69**(13):(134106).
- [13] Yamaguchi, M., M. Shiga et al. Grain boundary decohesion by sulfur segregation in ferromagnetic iron and nickel-a first-principles study. *Materials Transactions*. 2006;**47**(11):(2682–2689).
- [14] Rose, J. H., J. Ferrante and J. R. Smith. Universal binding energy curves for metals and bimetallic interfaces. *Physical Review Letters*. 1981;**47**(9):(675–678).
- [15] Mott, N. F. The electrical conductivity of transition metals. *Proceedings of the Royal Society of London. Series A, Mathematical and Physical Sciences*. 1936;**153**(880):(699–717).
- [16] Chen, L., et al. First-principle investigation of bismuth segregation at  $\Sigma 5$  (210) grain-boundaries in nickel. *Transactions of Nonferrous Metals Society of China*. 2006;**16**(Supplement 2(0)):(s813–s819).
- [17] Yamaguchi, M., M. Shiga and H. Kaburaki. Grain boundary decohesion by impurity segregation in a nickel-sulfur system. *Science*. 2005;**307**(5708):(393–397).
- [18] Kart, H. H., T. Cagin. The effects of boron impurity atoms on nickel  $\Sigma 5$  (210) grain boundary by first principles calculations. *JAMME*. 2008;**30**(2008):(177–181).
- [19] Geng, W. T., A. J. Freeman, R. Wu, C. B. Geller and J. E. Reynolds. Embrittling and strengthening effects of hydrogen, boron, and phosphorus. *Physical Review B*. 1999;**60**(10):(7149–7155).
- [20] Masatake, Y., S. Motoyuki and K. Hideo. Energetics of segregation and embrittling potency for non-transition elements in the Ni  $\Sigma 5$  (012) symmetrical tilt grain boundary: a first-principles study. *Journal of Physics: Condensed Matter*. 2004;**16**(23):(3933).

- [21] Bricknell, R. H., and D. A. Woodford. The embrittlement of nickel following high temperature air exposure. *Metallurgical Transactions A*. 1981;**12(3)**:(425–433).
- [22] Sims, C. T. A history of superalloy metallurgy for superalloy metallurgists. *Superalloys*. 1984;**1984**:(399–419).
- [23] Sanyal, S., U. V. Waghmare, P. R. Subramanian and M. F. X. Gigliotti. Effect of dopants on grain boundary decohesion of Ni: a first-principles study. *Applied Physics Letters*. 2008;**93(22)**:(223113).
- [24] Young, G., R. Najafabadi et al. Applications of Ab Initio Modeling to Materials Science: Grain Boundary Cohesion and Solid State Diffusion. 2004;No. LM-04K037. Lockheed Martin Corporation, NY, US.
- [25] Lejček, P., et al. Why calculated energies of grain boundary segregation are unreliable when segregant solubility is low. *Scripta Materialia*. 2013;**68(8)**:(547–550).
- [26] Jena, A. K. and M. C. Chaturvedi. The role of alloying elements in the design of nickel-base superalloys. *Journal of Materials Science*. 1984;**19(10)**:(3121–3139).
- [27] Tahir, A. M. Development and validation of a scale-bridging method for simulation of intergranular fracture in body centered cubic metals. ICAMS 2014 (thesis).
- [28] Bentria, E. T., I. K. Lefkaier, and B. Bentria. The effect of vanadium impurity on Nickel  $\Sigma 5(012)$  grain boundary. *Materials Science and Engineering A*. 2013;**577**:(197–201).
- [29] Tyson, W. and W. Miller. Surface free energies of solid metals: estimation from liquid surface tension measurements. *Surface Science*. 1997;**62(1)**:(267–276)
- [30] Zhang, L., X. Shu, S. Jin, Y. Zhang and G. -H. Lu. First-principles study of He effects in a bcc Fe grain boundary: site preference, segregation and theoretical tensile strength. *Journal of Physics: Condensed Matter*. 2010;**22(37)**:(375401)
- [31] Donald J. Siegel, J.C. Hamilton. Computational study of carbon segregation and diffusion within a nickel grain boundary. *Acta Materialia*. 2005;**53**:(87–96).

